DOI: 10.1002/anie.200((will be filled in by the editorial staff))

The Final Piece of the Puzzle: The Solid-State Structure of SF_4

*James T. Goettel, Nathan Kostiuk, and Michael Gerken**

Sulfur tetrafluoride is one of the fundamental binary main-group fluorides and, since its discovery in 1929,[1] its structure and chemistry, particularly as a fluorinating agent in organic chemistry, has been subject to many studies.[2] The structure of SF_4 has been determined in the gas phase by microwave spectroscopy[3] and electron diffraction,[4] revealing its molecular seesaw geometry (C_{2v}), which is in accord with the VSEPR model. Vibrational spectra of liquid SF_4 have also been assigned in terms of molecular C_{2v} point symmetry.[5] Sulfur tetrafluoride is one of the typical examples for a fluxional trigonal bipyramidal geometry, with rapidly exchanging axial and equatorial fluorine environments on the NMR time scale at room temperature.[6] At low-temperature, the exchange can be slowed down, allowing the observation of two triplets in the ^{19}F NMR spectrum. The exchange of axial and equatorial fluorine environments of pure SF_4 has been shown to proceed via Berry pseudorotation with activation energies of 11.9 (gas phase) and 11.2 (liquid, solution) kcal mol^{-1}.[6] An NMR study of the temperature dependence of the ^{19}F NMR chemical shifts and ^2J coupling constants suggested the presence of labile fluorine bridging with the possibility of dimer or chain formation being discussed.[7] Solid-state Raman spectroscopic data have been interpreted in terms of three different polymorphs, suggesting fluorine-bridged chains for the solid-state structure of SF_4.[8] Using miniature zone-melting techniques, the crystal structure of SF_4 has previously been reported to be severely disordered and no discernible structure could be determined.[9] Despite the broad interest in the structure of SF_4, its solid-state structure has remained elusive as a consequence of its low melting point and highly reactive nature. The crystal structures of SeF_4 and TeF_4, on the other hand, have previously been obtained.[10] Tellurium tetrafluoride exists as TeF_3 units bridged by two fluorides, whereas SeF_4 contains distinct disphenoidal SeF_4 units, having Se···F contacts to two adjacent SeF_4 molecules.

In the present study, we were able to obtain crystals of SF_4, which has a melting point of –121 °C, using two different methods: (a) by slow cooling of neat liquid SF_4 and (b) by crystallization from CF_2Cl_2 solvent. Both types of crystals were mounted at –145 °C and shown to have the same unit cell. The initial data suggested a tetragonal unit cell. The correct structural solution, however, showed that SF_4 crystallized in the orthorhombic system with merohedral twinning and two crystallographically unique ordered SF_4 molecules in the asymmetric unit. In our study, we did not find any evidence for a polymorph of SF_4.

The geometry of the SF_4 molecules agrees well with the seesaw geometry found for the gas phase.[3,4] The axial S–F bonds are longer (1.635(4) – 1.671(5) Å) and more ionic in nature than the shorter equatorial S–F bonds (1.474(6) – 1.553(4) Å). The axial and equatorial F–S–F angles found in the solid-state structure are indistinguishable from those of the gas-phase structure. The extended structure can be described as a 3-dimensional network of SF_4 molecules linked by two weak intermolecular S···F contacts per SF_4 molecule. The shortest S···F contact found in the structure is 2.954(5) Å, which is shorter than the sum of the van-der-Waals radii (3.27 Å).[11] These contacts are exclusively formed by the more ionic axial fluorines to the sulfur atoms of adjacent SF_4 molecules. None of the equatorial fluorines form significant intermolecular contacts. This agrees very well with the more covalent nature of the S–F_{eq} bonds and the lower fluorobasicity of the equatorial fluorines compared to the axial fluorines. Because of the location of the lone pair in the F_{eq}–S–F_{eq} plane, the F···S···F angles (121.2(2)° and 116.2(1)°) are significantly larger than the F_{eq}–S–F_{eq} angles (101.0(2)° and 99.6(3)°). The weakness of the contacts is reflected in the low freezing point of SF_4 and the fact that the gas-phase and solid-phase metric parameters of the SF_4 molecule are the same within the experimental errors. The structures of SF_4 and SeF_4 are related in respect that both contain contacts between the axial fluorines and the chalcogens resulting in a fluorine-bridged network. In SF_4, however, only three of the four crystallographically different axial fluorine atoms form contacts, while in SeF_4 all axial fluorines form Se–F···Se bridges.

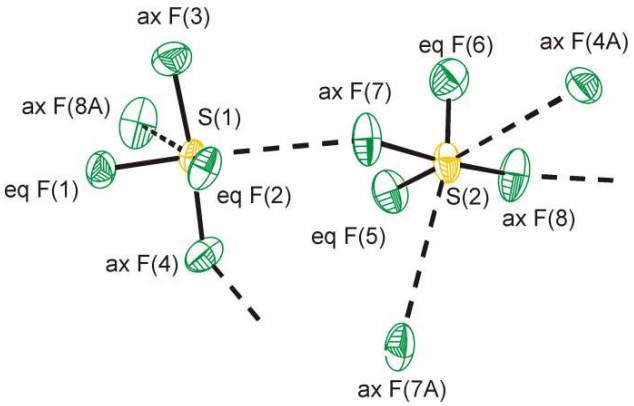

Figure 1. Thermal ellipsoid plot of the SF_4. Thermal ellipsoids are set at 50 % probability. Selected bond lengths (Å), contacts (Å), and angles (°): S(1)–F(1) 1.527(4); S(1)–F(2) 1.535(4); S(1)–F(3) 1.647(5); S(1)–F(4) 1.676(5); F(1)–S(1)–F(2) 101.0(2); F(3)–S(1)–F(4) 172.6(3); S(1)···F(7) 2.954(5); S(1)···F(8A) 3.031(5); F(7)···S(1)···F(8A) 121.2(2); S(2)–F(5) 1.553(4); S(2)–F(6) 1.474(6); S(2)–F(7) 1.671(5); S(2)–F(8) 1.635(4); F(5)–S(2)–F(6) 99.6(3); F(7)–S(2)–F(8) 171.6(3); S(2)···F(4A) 2.975(4); S(2)···F(7A) 3.261(6); F(4A)···S(2)···F(7A) 116.2(1).

A solid-state structural motif similar to that of neat SF_4 is observed in the crystal structure of the novel $[HNC_5H_3(CH_3)_2^+]_2F^-\cdots SF_4[SF_5^-]\cdot 3SF_4$ salt. Excess SF_4 reacts with a mixture of water and 2,6-dimethylpyridine, yielding a white

[*] James T. Goettel, Nathan Kostiuk, Prof. Dr. Michael Gerken
Department of Chemistry and Biochemistry
University of Lethbridge
4401 University Drive, Lethbridge, Alberta T1K 3M4
Fax: (+) 403-329-20576
E-mail: michael.gerken@uleth.ca

[**] This work was funded by the Natural Sciences and Engineering Research Council of Canada (NSERC).

Supporting information for this article is available on the WWW under http://www.angewandte.org or from the author.

crystalline solid according to equation (1). The $[HNC_5H_3(CH_3)_2^+]_2F^-\cdots SF_4[SF_5^-]\bullet 3SF_4$ salt is stable up to –90 °C, above which the crystals decompose.

$$6SF_4 + H_2O + 2N(C_5H_3)(CH_3)_2 \longrightarrow [HNC_5H_3(CH_3)_2^+]_2F^-\cdots SF_4[SF_5^-]\bullet 3SF_4 + SOF_2 \quad (1)$$

The asymmetric unit of $[HNC_5H_3(CH_3)_2^+]_2F^-\cdots SF_4[SF_5^-]\bullet 3SF_4$ contains (i) two 2,6-dimethylpyridinium cations that are hydrogen-bonded to a fluoride anion, (ii) an SF_5^- anion (Figure 2), and (iii) four crystallographically different SF_4 molecules. Two different interaction modalities between F^- and SF_4 are present in this structure. The fluoride-ion acceptor properties of SF_4 towards F^- has been established by the formation of salts containing the SF_5^- anion[12] and recently, the Lewis-acidity of SF_4 towards organic bases has conclusively been shown for the base $N(C_2H_5)_3$.[13]

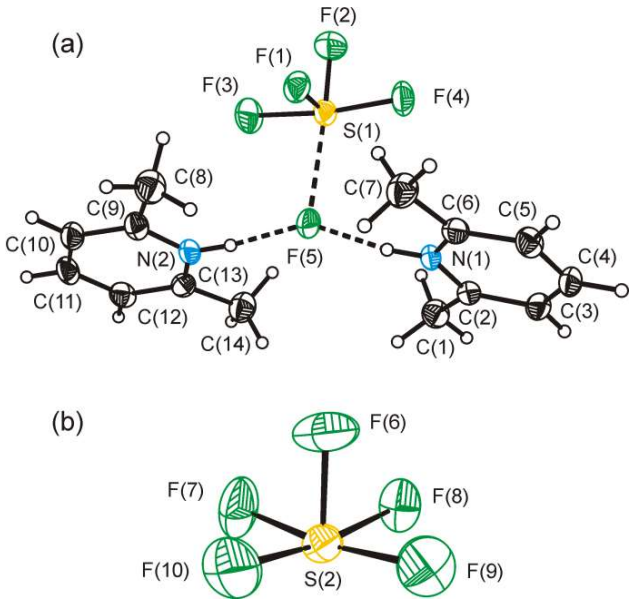

Figure 2. Thermal ellipsoid plot of the (a) $[HNC_5H_3(CH_3)_2^+]_2F^-\cdots SF_4$ moiety and (b) the SF_5^- anion in $[HNC_5H_3(CH_3)_2^+]_2F^-\cdots SF_4[SF_5^-]\bullet 3SF_4$. Thermal ellipsoids are set at 50 % probability. Selected bond lengths (Å), contacts (Å), and angles (°): S(1)–F(1) 1.549(2); S(1)–F(2) 1.545(2); S(1)–F(3) 1.650(2); S(1)–F(4) 1.706(2); S(1)···F(5) 2.487(2); F(5)···N(1) 2.554(3); F(5)···N(2) 2.553(3); S(2)–F(6) 1.564(2); S(2)–F(7) 1.730(2); S(2)–F(8) 1.763(2); S(2)–F(9) 1.719(2); S(2)–F(10) 1.664(2); F(7)–S(2)–F(9) 171.086(13); F(8)–S(2)–F(10) 170.70(13).

In the present structure, the fluoride which is hydrogen-bonded to two 2,6-dimethylpyridinium cations forms F···S(1) contacts (2.487(2) Å) with one SF_4 molecule. These contacts are significantly stronger than the F···S contacts found in solid SF_4, resulting in an increase of the average S–F bond lengths in the $F^-\cdots SF_4$ moiety. The effect of coordination of fluoride on the structure of SF_4 in this salt, however, is less pronounced than that of $N(C_2H_5)_3$ coordination observed in the structure of $SF_4\cdot N(C_2H_5)_3$,[13] reflecting the weaker interaction between SF_4 and a fluoride that is hydrogen-bonded to two cations. A second significantly weaker interaction between sulfur and a fluorine atom from the SF_5^- anion expands the coordination environment about S(1) to six. The second fluoride ion in the structure is sufficiently naked to form the SF_5^- anion, which adopts the expected square pyramidal structure. Besides $Rb[SF_5]$, $Cs_6[SF_5]_4[HF_2]_2$,[12d] and $[Cs(18\text{-crown-}6)_2][SF_5]$,[12e] this is the fourth structurally characterized salt containing the SF_5^- anion. Because three of the four equatorial fluorine atoms of this anion form F···S contacts, the anion is locked into one position without being disordered. As a consequence of the contacts the anion geometry deviates from an idealized square pyramid. As expected, the axial S–F bond (1.564(2) Å) is much shorter than the equatorial S–F bonds (1.664(2) to 1.763(2) Å). The three equatorial fluorines that have contacts to adjacent SF_4 molecules have significantly longer S–F bonds (1.719(2) – 1.763(2) Å) than the bond to the other equatorial fluorine, which does not form contacts. The average of the equatorial S–F bond lengths is 1.719 Å, which is in excellent agreement with the average equatorial bond length reported for $Rb[SF_5]$ (1.718 Å). Moreso, the average of each pair of equatorial S–F bond lengths that are trans to each other gives this value within the experimental error. The fluorine in SF_5^- that forms the strongest contact, i.e., F(8), has the longest and most ionic S–F bond and is trans to the shortest most covalent equatorial bond, i.e., S(2)–F(10). As mentioned for the anion in $Rb[SF_5]$,[12d] the presence of the lone pair on sulfur results in sulfur being 0.136 Å below the plane formed by the four equatorial fluorine atoms.

The packing of $[HNC_5H_3(CH_3)_2^+]_2F^-\cdots SF_4[SF_5^-]\bullet 3SF_4$ shows two distinct layers along the *ab* plane. The SF_4 molecule that exhibits S···F contacts to the fluoride is located within a layer of the $[HNC_5H_3(CH_3)_2^+]$ cations and the F^- and SF_5^- anions. The other three SF_4 molecules form a layer separating two ionic layers (Figure 3). The two types of SF_4 molecules show significant differences in the size of their fluorine thermal ellipsoids, i.e., the SF_4 coordinated to F^- exhibits smaller thermal parameters, than the fluorines of the 'free' SF_4, reflecting significantly more thermal motion. This is paralleled by the relatively large thermal ellipsoids found in solid SF_4 at –173 °C. The coordination environments about sulfur in all SF_4 molecules include two S···F contacts (Figure S3), which is similar to the coordination environment found in solid neat SF_4. The contacts involving fluorines from the SF_5^- anion (2.755(2) to 2.937(2) Å) are in general shorter than those from fluorines of adjacent SF_4 molecules (2.867(2) to 3.164(3) Å), reflecting the larger fluorobasicity of the anions. The $F_4S\cdots FSF_3$ contacts are similar to those found in the structure of neat SF_4. As shown in Figure 3, the SF_4 molecules in the layer form contacts to molecules within the layer, as well as to the adjacent ionic layers, holding the layers together.

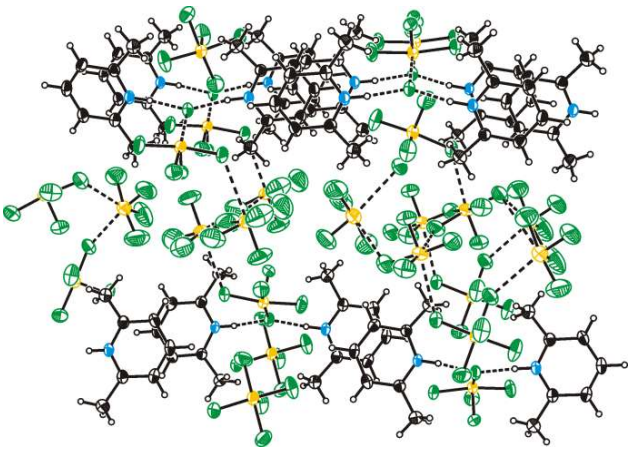

Figure 3. Thermal ellipsoid view along the *a*-axis of the packing of $[HNC_5H_3(CH_3)_2^+]_2F^-\cdots SF_4[SF_5^-]\bullet 3SF_4$. Thermal ellipsoids are set at 50 % probability.

The Raman spectrum of solid SF_4 exhibits significant splitting as previously observed.[8] These splittings can be explained by the presence of two crystallographically different SF_4 molecules and/or by vibrational coupling between SF_4 molecules in one unit cell. The Raman spectrum of $[HNC_5H_3(CH_3)_2^+]_2F^-\cdots SF_4[SF_5^-]\bullet 3SF_4$ at −100 °C is depicted in Figure 4 and contains the characteristic signals associated with the $HNC_5H_3(CH_3)_2^+$ cation and the SF_5^- anion. The latter were assigned based on the vibrational assignments previously reported for the Cs^+ and $[Cs(18\text{-crown-}6)_2]^+$ salts.[12] The Raman spectrum also shows several bands attributable to SF_4. Interestingly, two sets of bands in the equatorial SF_2 stretching region can be distinguished and tentatively assigned to $\nu_s(SF_{2,eq})$ of SF_4 in the layer (880 cm^{-1}), which is close to that of neat solid SF_4 (888, 879 cm^{-1}), and that of SF_4 coordinated by F^- (863 cm^{-1}) (Table S1). A Raman spectrum of solid $[HNC_5H_3(CH_3)_2^+]_2F^-\cdots SF_4[SF_5^-]\bullet 3SF_4$ recorded at −85 °C contains a broadened signal at 884 cm^{-1}, which resembles the broad signal observed in liquid SF_4. This observation corroborates the observation of significant thermal motion within the SF_4 layer and suggests the onset of decomposition via release of SF_4.

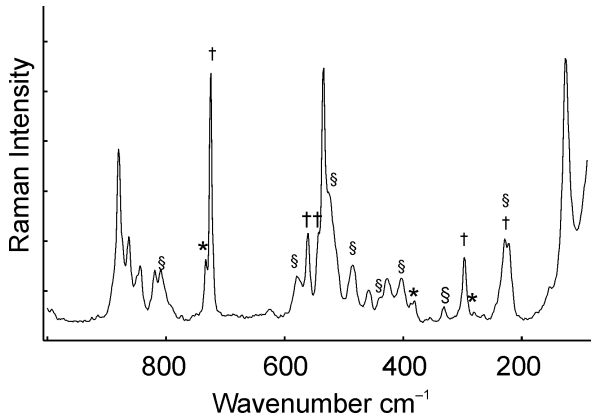

Figure 4. Raman spectrum of $[HNC_5H_3(CH_3)_2^+]_2F^-\cdots SF_4[SF_5^-]\bullet 3SF_4$ at −100 °C. Asterisks (*) denote bands arising from the FEP sample tube. Bands attributed to the 2,6-dimethylpyridinium cation and to the SF_5^- anion are denoted by (†) and (§), respectively.

In conclusion, for the first time, the structure of SF_4 in the solid state has been elucidated. The structure can best be described as a network with weak intermolecular S···F contacts formed exclusively with the axial fluorines that exhibit more ionic character. The structure is different from previous predictions of chain-type or dimeric structures, which contains two contacts between each SF_4 molecule.[7] A similar structural motif is found in the novel $[HNC_5H_3(CH_3)_2^+]_2F^-\cdots SF_4[SF_5^-]\bullet 3SF_4$ salt which contain SF_4 layers. As in neat SF_4, the SF_4 molecules within the layer of the salt have two S···F contacts of similar distances and do not form distinct dimers or chains. Because of the weakness of interactions, the overall structure, i.e., network versus layer, greatly depends on the nature of composition of the compound. The $[HNC_5H_3(CH_3)_2^+]_2F^-\cdots SF_4[SF_5^-]\bullet 3SF_4$ salt represents the first compound that contains a range of interaction motifs between SF_4 and F, i.e., $F_4S\text{–}F^-$ (1.564(2) to 1.763(2) Å), $F_4S\cdots F^-$ (2.587(2) Å), $F_4S\cdots FSF_4^-$ (1.755(2) to 2.937(2) Å), $F_4S\cdots FSF_3$ (2.867(2) to 3.164(2) Å).

Experimental

General: All volatile materials were handled on a vacuum line constructed of nickel, stainless steel, and FEP. Reaction vessels were fabricated from ¼-in. o.d. FEP tubing and outfitted with Kel-F valves. All reaction vessels were rigorously dried under dynamic vacuum followed by treatment with > 1 atm of F_2 gas.

Sulfur tetrafluoride (Ozark-Mahoning Co.) was purified by passing the gas through a column of activated charcoal. Traces of thionyl fluoride and sulfur hexafluoride were present in the sulfur tetrafluoride, but did not interfere with the chemistry. Difluorodichloromethane (Synquest Labs Inc.), 2,6-dimethylpyridine (Sigma-Aldrich) were used as received.

Synthesis of $[HNC_5H_3(CH_3)_2^+]_2F^-\cdots SF_4[SF_5^-]\bullet 3SF_4$: Water (0.016 g, 0.89 mmol) was injected into a ¼-in. FEP reactor equipped with a Kel-F valve using a micro syringe. 2,6-dimethylpyridine (0.176 g, 1.64 mmol) was then injected into the ¼-in. FEP reactor in a dry nitrogen filled glove bag. A large excess of SF_4 was vacuum-distilled onto the frozen mixture at –196 °C. Upon melting of SF_4 at –120 °C, a vigorous reaction occurred, causing a white insoluble precipitate to form. Warming the reaction mixture to 0 °C formed a clear colourless solution. Upon cooling of this solution to –85 °C large needles formed. Excess SF_4 was partially removed under dynamic vacuum at –95 °C, yielding 0.691 g of a white solid, i.e., $[HNC_5H_3(CH_3)_2^+]_2F^-\cdots SF_4[SF_5^-]\bullet 3SF_4$ with small amounts of residual SF_4.

Raman spectroscopy All Raman spectra were recorded on a Bruker RFS 100 FT Raman spectrometer with a quartz beam splitter, a liquid-nitrogen cooled Ge detector, and R-496 temperature accessory. The actual usable Stokes range was 50 to 3500 cm^{-1}. The 1064-nm line of an Nd:YAG laser was used for excitation of the sample. The Raman spectra were recorded at –110 °C with a spectral resolution of 2 cm^{-1} using laser powers of 300 mW.

X-ray crystallography: F_4S: formula weight M_r = 108.06 g cm^{-3}, clear colourless plate (0.17 × 0.15 × 0.14 mm^3), orthorhombic, $P2_12_12_1$, Z = 8, a = 6.773(4), b = 6.812(4), c = 13.122(8) Å, V = 605.5(6) Å ^{3}, ρ_{calcd} = 2.371 gcm^{-3}, $2\theta_{max}$ 54.4°, $\lambda(Mo_{K\alpha})$ = 0.71073 Å, 100(2) K, 6874 reflections, 1387 unique reflections (R_{int} = 0.052), absorption coefficient (μ = 0.98 mm^{-1}), R_1 = 0.050, wR_2= 0.112.

$C_{14}H_{20}F_{22}N_2S_5$: formula weight M_r = 794.61 g cm^{-3}, clear colourless block (0.16 × 0.19 × 0.57 mm^3), orthorhombic, $P2_12_12_1$, Z = 4, a = 7.4597(10), b = 18.150(2), c = 21.863(3) Å, V = 2960.2(7) Å ^{3}, ρ_{calcd} = 1.783 gcm^{-3}, $2\theta_{max}$ = 55.2°, $\lambda(Mo_{K\alpha})$ = 0.71073 Å, 133(2) K, 33934 reflections, 6819 unique reflections (R_{int} = 0.033), absorption coefficient (μ = 0.54 mm^{-1}), R_1 = 0.042, wR_2= 0.117.

The crystals were mounted at low temperature under a stream of cold dry nitrogen as previously described.[14] The crystals were centered on a Bruker SMART APEX II diffractometer, controlled by the APEX2 Graphical User Interface software.[15] The program SADABS[16] was used for scaling of diffraction data, the application of a decay correction, and a multi-scan absorption correction. Program SHELXS-97[17] was used for both solution and refinement. A structure solution was obtained by direct methods. CSD 425996 (SF_4) and CCDC 932409 ($C_{14}H_{20}F_{22}N_2S_5$) contain the supporting crystallographic data; these data can be obtained free of charge from the Fachinformationszentrum Karlsruhe (SF_4) via http://www.fiz-karlsruhe.de/request_for_deposited_data.html) and The Cambridge Crystallographic Data Centre ($C_{14}H_{20}F_{22}N_2S_5$) via www.ccdc.cam.ac.uk/data_request/cif.

Received: ((will be filled in by the editorial staff))
Published online on ((will be filled in by the editorial staff))

Keywords: sulfur tetrafluoride · fluorine · crystallography · Raman spectrosocpy

[1] J. Fischer and W. Jaenckner, *Angew. Chem.* **1929**, *42*, 810-811.
[2] a) W. C. Smith, *Angew. Chem.* **1962**, *74*, 742-751; b) W. Dmowski, in *Houben-Weyl, Organo-Fluorine Compounds* Vol. E10a (Eds.: B. Baasner, H. Hagemann, J. C. Tatlow), Thieme, Stuttgart, **2000**, Chapter 8; c) H. Oberhammer, S. A. Shykov, *Dalton Trans.* **2010**, *39*, 2838-2841.
[3] W. M. Tolles and W. D. Gwinn, *J. Chem. Phys.*, **1962**, *36*, 1119-1121.
[4] a) K. Kimura and S. H. Bauer, *J. Chem. Phys.*, **1963**, *39*, 3172-3178; b) V. C. Ewing and L. E. Sutton, *Trans. Faraday Soc.*, **1963**, *59*, 1241-1247.
[5] K. O. Christe, X. Zhang, J. A. Sheehy, R. Bau, *J. Am. Chem. Soc.* **2001**, *123*, 6338-6348, and references therein.

[6] a) A. N. Taha, N. S. True, C. B. LeMaster, C. L. LeMaster, S. M. Neugebauer-Crawford, *J. Chem. Phys. A* **2000,** *104*, 3341-3348; b) F. Seel, W. Gombler, *J. Fluorine Chem.* **1974**, *4*, 327-331.
[7] W. Gombler, F. Seel, *J. Fluorine Chem.* **1974**, *4*, 333-339
[8] a) C. V. Berney, *J. Mol. Struct.* **1972**, *12,* 87-97; b) K. O. Christe, E. C. Curtis, C. J. Schack, S. J. Cyvin, J. Brunvoll, W. Sawodny, *Spectrochim. Acta* **1976**, *32A*, 1141-1147.
[9] D. Mootz, L. Korte, *Z. Naturforsch.* **1984**, *39b*, 1295-1299
[10] R. Kniep, L. Korte, R. Kryschi, W. Poll, *Angew. Chem. Int. Ed. Engl.* **1984** , *23*, 388-389
[11] A. Bondi, *J. Phys. Chem.* **1964**, *68*, 441-451.
[12] a) R. Tunder, B. Siegel, *J. Inorg. Nucl. Chem.* **1963**, *25*, 1097-1098; b) K. O. Christe, E. C. Curtis, C. J. Schack, D. Pilippovich, *Inorg. Chem.* **1972**, 11, 1679-1682 c) L. F. Drullinger, J. E. Griffiths, *Spectrochim. Acta, Part A* **1971**, 27a, 1793-1799; d) J. Bittner, J. Fuchs, K. Seppelt, *Z. Anorg. Allg. Chem.* **1988**, 557, 183-190; e) M. Clark, C. J. Kellen-Yuen, K. D. Robinson, H. Zhang, Z. Y. Yang, K. V. Madappat, J. W. Fuller, J. L. Atwood, and J. S. Thrasher, *Eur. J. Solid State Inorg. Chem.* **1992**, 29, 809-833.
[13] J. T. Goettel, P. Chaudhary, P. Hazendonk, H. P. A. Mercier, M. Gerken, *Chem. Commun.* **2012**, *48*, 9120-9122.
[14] M. Gerken, D. A. Dixon, G. J. Schrobilgen, *Inorg. Chem.* **2000**, *39*, 4244-4255.
[15] *APEX* 2, Version 2.2-0; Bruker AXS Inc.: Madison, WI, **2007**.
[16] G. M. Sheldrick, *SADABS*, Version 2007/4; Bruker AXS Inc.; Madison, WI, **2007**.
[17] G. M. Sheldrick, *SHELXTL97*, University of Göttingen, Germany, **2007**.

Entry for the Table of Contents (Please choose one layout)

Layout 1:

Sulfur tetrafluoride

J. T. Goettel, N. Kostiuk, M. Gerken*__ **Page – Page**

The Final Piece of the Puzzle: The Solid-State Structure of SF_4

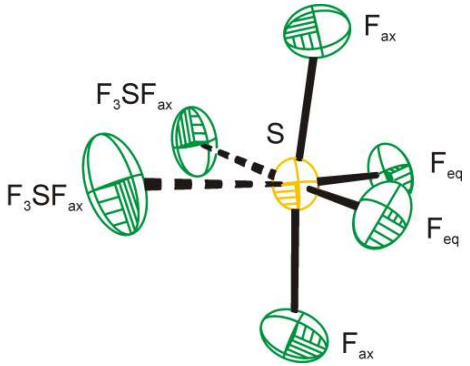

Structural elucidation: The crystal structure of solid SF_4, which has a melting point of –121 °C, was obtained, exhibiting weak intermolecular S···F interactions. A similar structural motif was observed within a layer of SF_4 in $[HNC_5H_3(CH_3)_2^+]_2F^-\cdots SF_4[SF_5^-]\cdot 3SF_4$. The latter structure contains a range of bonding modalities between S and F, i.e., SF_5^-, $F_4S\cdots F^-$, $F_4S\cdots FSF_4^-$, $F_4S\cdots FSF_3$.

Layout 2:

((Author(s), Corresponding Author(s)*))
_____ **Page – Page**

((Title Text))

((TOC Graphic))

Supporting Information

Crystal Growth and Crystal Mounting:

Neat SF_4: Sulfur tetrafluoride (0.015 g, 1.4 mmol) was vacuum distilled into a ¼-in. o.d. FEP reactor. Crystals were grown by slowly cooling the liquid SF_4 to –150 °C in the ¼-in FEP reactor placed on an aluminium cold trough. After the temperature stabilized, the FEP tube was cut approximately 6 cm above the frozen SF_4. A Pasteur pipette was used to remove some crystals. A suitable crystal (0.063 × 0.075 × 0.117 mm^3) was affixed to a nylon cryo-loop coated in Fomblin Z-15 perfluorinated oil. Crystals were mounted at low temperature under a stream of dry cold nitrogen as previously described.[1]

SF_4 in CF_2Cl_2: Sulfur tetrafluoride (0.034 g, 3.1 mmol) was vacuum distilled in a ¼-in. o.d. FEP reactor. Approximately 0.1 mL of CF_2Cl_2 was vacuum distilled on top of the solid SF_4. Upon melting, two distinct layers were observed. Agitation caused the liquids to mix. Cooling of the solution to –131.8 °C and reducing the volume of CF_2Cl_2 under dynamic vacuum led to the formation of plate-shaped crystals. The FEP was cut in a cold trough, and the crystals were removed using a Pasteur pipette. A suitable plate (0.135 × 0.149 × 0.173 mm^3) was affixed to a droplet of Fomblin Z-15 perfluorinated oil on a nylon cryo-loop.

$[HNC_5H_3(CH_3)_2^+]_2F^- \cdots SF_4[SF_5^-] \cdot 3SF_4$: Crystals were mounted in a similar fashion as SF_4. A sticky mass of crystals were transferred from the ¼-in. o.d. FEP tube to an FEP platform with the help of a Pasteur pipette. A block (0.162 × 0.191 × 0.576 mm^3) was mounted on a droplet of perfluorinated Z-15 oil affixed to a nylon cryo-loop. Four crystals were mounted; each had the same unit cell.

---

[1] M. Gerken, D. A. Dixon, G. J. Schrobilgen, *Inorg. Chem.* **2000**, *39*, 4244-4255.

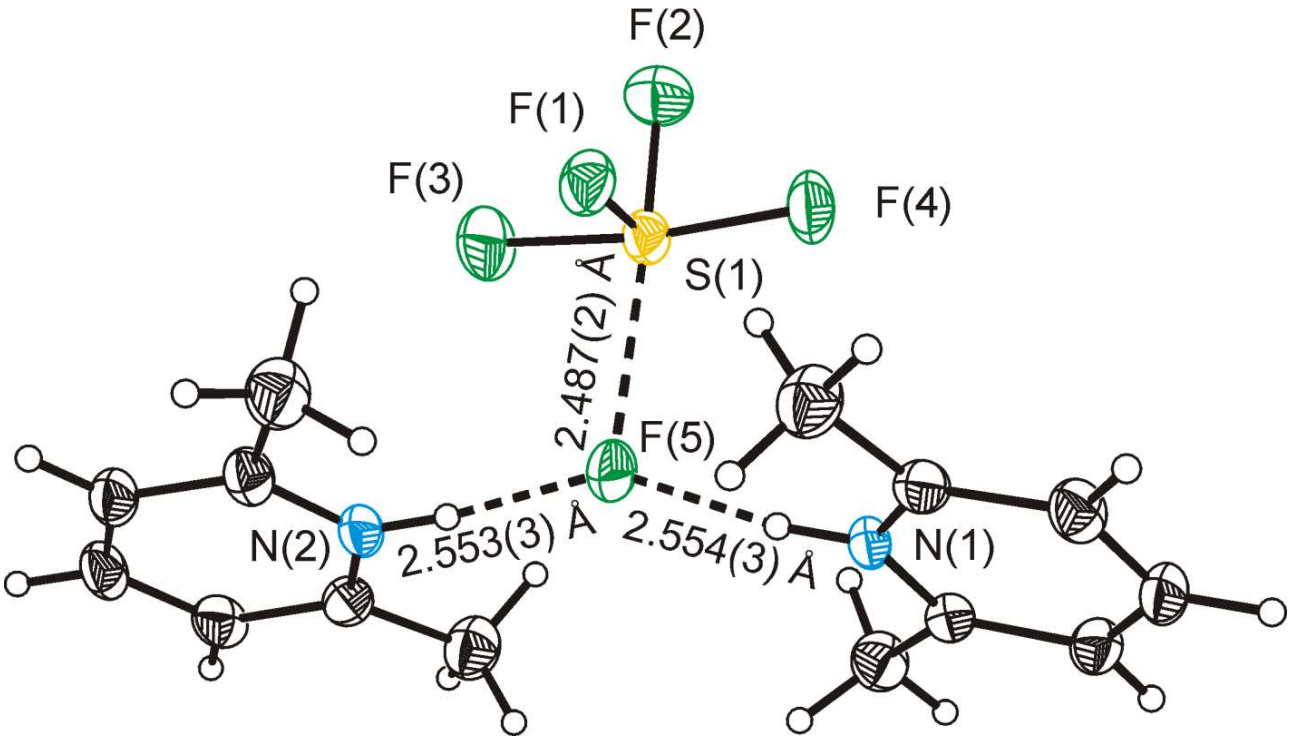

Figure S1 Thermal ellipsoid plot of the $[HNC_5(CH_3)_2H_3^+]_2F^-$ moiety in the X-ray crystal structure of $[HNC_5H_3(CH_3)_2^+]_2F^-\cdots SF_4[SF_5^-]\bullet 3SF_4$; thermal ellipsoids are drawn at the 50% probability level.

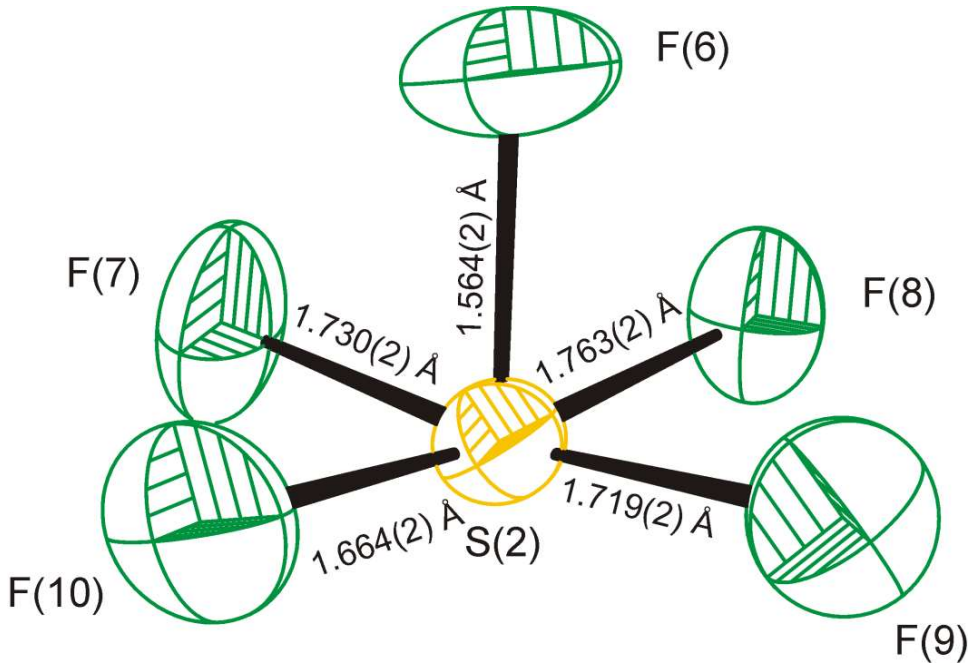

Figure S2 Thermal ellipsoid plot of the SF_5^- anion in the X-ray crystal structure of $[HNC_5H_3(CH_3)_2^+]_2F^-\cdots SF_4[SF_5^-]\bullet 3SF_4$; thermal ellipsoids are drawn at the 50% probability level.

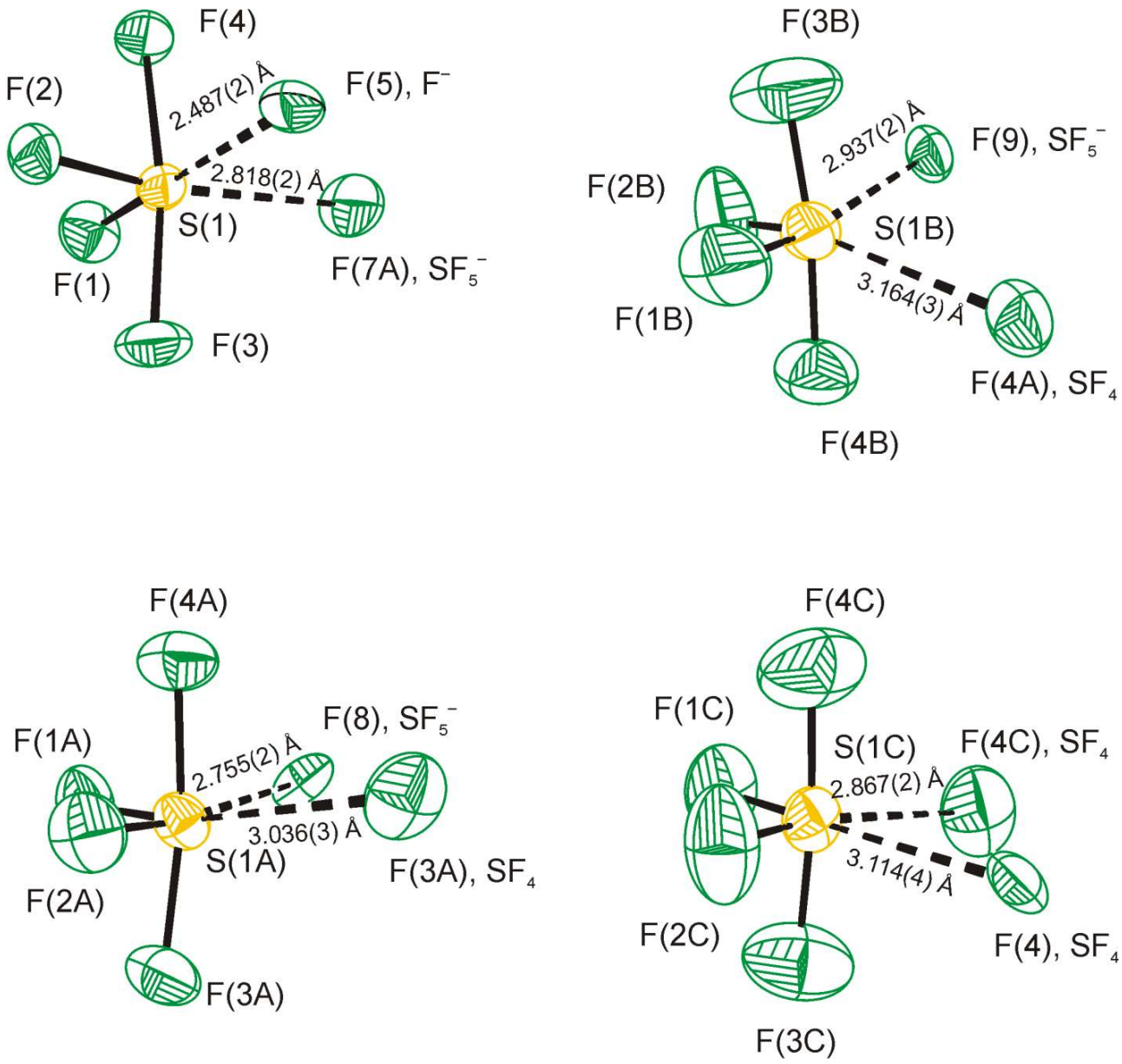

Figure S3 Thermal ellipsoid plot of the coordination environment about the SF_4 molecules in the X-ray crystal structure of $[HNC_5H_3(CH_3)_2^+]_2F^-\cdots SF_4[SF_5^-]\bullet 3SF_4$; thermal ellipsoids are drawn at the 50% probability level.

Table S1 Experimental Raman frequencies for $[HNC_5H_3(CH_3)_2^+]_2F^-\cdots SF_4[SF_5^-]\bullet 3SF_4$

$[HNC_5H_3(CH_3)_2^+]_2F^-\cdots SF_4[SF_5^-]\bullet 3SF_4$[a]		SF_4 solid[b]		SF_5^- in $CsSF_5$[c]/$[Cs(18\text{-crown-}6)_2]SF_5$ [d]	
	Assignment		Assignment		Assignment
3111(6)					
3082(6)	ν(C–H)				
3015(6)					
2981(13)					
2940(66)	$\nu(CH_3)$				
2861(3)					
2757(8)					
1657(10)					
1626(20)	ν(C–C)/ ν(C–N)				
1556(7)					
1439(6)					
1420(9)					
1393(30)	CH_3 deform				
1385(31)	CH_3 deform				
1312(4)					
1293(27)	ν(C–C) / ν(C–N)				
1286sh					
1216(3)					
1174(9)					
1100(16)	$\nu_s(NC_5)$				
1089(4)					
1015(86)					
993(5)					
		901	Overtone or combination band		
880(63)	SF_4 (in layer), $\nu_s(SF_{2eq})$	888 879	$\nu_s(SF_{2eq})$		
863(32)	$SF_4\cdots F^-$, $\nu_s(SF_{2eq})$				
849sh 844(21)	SF_4 (in layer), $\nu_{as}(SF_{2eq})$	860	$\nu_{as}(SF_{2eq})$		
819(19)	$SF_4\cdots F^-$,$\nu_{as}(SF_{2eq})$				
809(19) 803sh	SF_5^-, ν (SF_{ax})			796(37)/785(12)	ν (SF_{ax})
790sh					
725(90)	$\delta_{in\text{-}plane}$(CCC)/ $\delta_{in\text{-}plane}$(CNC)				
626(3)	SF_4, $\nu_{as}(SF_{2ax})$	650 623	$\nu_{as}(SF_{2ax})$		
580(16)[e] 574sh	SF_5^-, $\nu_{as}(SF_4)$			590 sh/583(7)	$\nu_{as}(SF_4)$
561(24)	$\delta_{in\text{-}plane}$(CCC)/ $\delta_{in\text{-}plane}$(CNC)				

543sh	$\delta_{in\text{-}plane}(CCC)/\ \delta_{in\text{-}plane}(NCC)$				
535(88)	$SF_4\ \nu_s(SF_{2ax})$	532	$\nu_s(SF_{2ax})$		
527sh 514sh	SF_4, $\delta_{rock}(SF_{2eq})$ $SF_5^-\ \nu_s(SF_4)$ in phase	524	$\delta_{rock}(SF_{2eq})$	522(27)/ 512(7)	$\nu_s(SF_4)$ in phase
486(16)	SF_4, $\delta_{sc}(SF_{2eq}) + \delta_{sc}(SF_{2ax})$ $SF_5^-\ \nu_s(SF_4)$ out of phase[e]	511 503	$\delta_{sc}(SF_{2eq}) + \delta_{sc}(SF_{2ax})$	435(100)[f]/469(100)	$\nu_s(SF_4)$ out of phase[g]
459(8)	SF_4, $\tau(SF_2)$	455	$\tau(SF_2)$		
440 sh	$SF_5^-\ \delta_s(SF_4)$ umbrella			469 sh/435(17)	$\delta_s(SF_4)$ umbrella
428(13)	$\delta_{out\text{-}of\text{-}plane}(CCH)$				
403(13)	SF_5^-, $\delta(F_{ax}SF_4)$ [e]	400		435(100)[f]/420(12)	$\delta(F_{ax}SF_4)$[g]
332(6)	SF_5^-, $\delta_s(SF_4)$ in plane	353	$\delta_{sc,\ out\ of\ plane}(SF_{2ax})$	342(16)/315(7)	$\delta_s(SF_4)$ in plane
297(23)[e]	$\rho_r(CH_3)$				
244sh 238sh	SF_4, $\delta_{sc}(SF_{2eq}) - \delta_{sc}(SF_{2ax})$ SF_5^-, $\delta_{as}(SF_4)$ out of plane	242	$\delta_{sc}(SF_{2eq}) - \delta_{sc}(SF_{2ax})$	269 sh/267(20)	$\delta_{as}(SF_4)$ out of plane
229(28) 222(27)	SF_5^-, $\delta_{as}(SF_4)$ in plane $\rho_r(CH_3)$			241(12)/242(13)	$\delta_{as}(SF_4)$ in plane
153(2) 126(100)	Lattice modes				

[a] Signals from the FEP sample tube were observed at 733(21), 387(4) 381(7), and 293sh cm^{-1}.

[b] From C. V. Berney, *J. Mol. Struct.* **1972**, *12*, 87-97 and K. O. Christe, E. C. Curtis, C. J. Schack, S. J. Cyvin, J. Brunvoll, W. Sawodny, *Spectrochim. Acta* **1976**, *32A*, 1141-1147.

[c] From K.O. Christe, E.C. Curtis, C. J. Schack, and D. Pilipovich, *Inorg. Chem.* **1972**, *11*, 1679-1682.

[d] From M. Clark, C. J. Kellen-Yuen, K. D. Robinson, H. Zhang, Z.-Y. Yang, K. V. Madappat, J. W. Fuller, J. L. Atwood, J. S. Thrasher, *Eur. J. Solid State Inorg. Chem.* **1992**, *29*, 809-833.

[e] Overlap with the FEP signal.

[f] Raman bands overlapped, resulting in an increased relative intensity.

[g] Assignment could be reversed.

Table S2 Metric parameters for SF_4.

Bond Lengths and Contacts, Å			
S1—F1	1.527 (4)	S2—F6	1.474 (6)
S1—F2	1.535 (4)	S2—F5	1.553 (4)
S1—F3	1.647 (5)	S2—F8	1.635 (4)
S1—F4	1.676 (5)	S2—F7	1.671 (5)
S1---F7	2.954 (5)	S2---F4^{ii}	2.975 (4)
S1---F8^{i}	3.031 (5)	S2---F7^{iii}	3.261 (6)
Bond Angles, deg.			
F1—S1—F2	101.0 (2)	F6—S2—F5	99.6 (3)
F1—S1—F3	88.3 (3)	F6—S2—F8	86.9 (3)
F2—S1—F3	87.7 (3)	F5—S2—F8	88.6 (3)
F1—S1—F4	87.3 (3)	F6—S2—F7	86.6 (3)
F2—S1—F4	87.3 (2)	F5—S2—F7	87.1 (3)
F3—S1—F4	172.6 (3)	F8—S2—F7	171.6 (3)
F1—S1---F7	170.4 (2)	F6—S2---F4^{ii}	73.8 (2)
F2—S1---F7	69.57 (18)	F5—S2---F4^{ii}	170.1 (3)
F3—S1---F7	92.9 (2)	F8—S2---F4^{ii}	83.6 (2)
F4—S1---F7	90.5 (2)	F7—S2---F4^{ii}	99.8 (2)
F1—S1---F8^{i}	68.4 (2)	F6—S2---F7^{iii}	167.3 (2)
F2—S1---F8^{i}	167.45 (19)	F5—S2---F7^{iii}	71.4 (2)
F3—S1---F8^{i}	85.4 (2)	F8—S2---F7^{iii}	101.5 (3)
F4—S1---F8^{i}	98.5 (2)	F7—S2---F7^{iii}	84.01 (18)
F7---S1---F8^{i}	121.21 (15)	F4^{ii}---S2---F7^{iii}	116.20 (13)
S2—F7---S1	135.9 (2)		

Symmetry codes: (i) −x+5/2, −y, z+1/2; (ii) x−1/2, −y+1/2, −z+2; (iii) x+1/2, −y+1/2, −z+2.

Table S3 Metric parameters for $[HNC_5H_3(CH_3)_2^+]_2F^-\cdots SF_4[SF_5^-]\bullet 3SF_4$

Bond Lengths and Contacts, Å			
S1—F1	1.5447 (18)	S1B---F9	2.937 (2)
S1—F2	1.549 (2)	S1B---F4A^{iii}	3.164 (3)
S1—F3	1.6503 (18)	S1C—F2C	1.502 (3)
S1—F4	1.7059 (18)	S1C—F1C	1.533 (2)
S1---F5	2.487 (2)	S1C—F3C	1.604 (3)
S1---F7^{i}	2.818 (2)	S1C—F4C	1.641 (4)
S1A—F1A	1.530 (2)	S1C---F4^{iv}	2.867 (2)
S1A—F2A	1.543 (2)	S1C---F4C^{v}	3.114 (4)
S1A—F3A	1.658 (2)	S2—F6	1.564 (2)
S1A—F4A	1.668 (2)	S2—F10	1.664 (2)
S1A---F8	2.755 (2)	S2—F9	1.719 (2)
S1A---F3A^{ii}	3.036 (3)	S2—F7	1.730 (2)
S1B—F2B	1.500 (4)	S2—F8	1.763 (2)
S1B—F1B	1.546 (3)	N1(H1)---F5	2.554 (3)
S1B—F3B	1.619 (3)	N2(H2)---F5	2.553 (3)
S1B—F4B	1.640 (3)		
Bond Angles, deg.			
F1—S1—F2	97.43 (11)	F2B—S1B---F9	75.21 (14)
F1—S1—F3	87.09 (11)	F1B—S1B---F9	172.89 (15)
F2—S1—F3	88.27 (12)	F3B—S1B---F9	86.07 (15)
F1—S1—F4	86.05 (10)	F4B—S1B---F9	100.26 (13)
F2—S1—F4	87.32 (11)	F2B—S1B---F4A^{iii}	168.7 (2)
F3—S1—F4	171.31 (11)	F1B—S1B---F4A^{iii}	76.38 (17)
F1—S1---F5	79.91 (9)	F3B—S1B---F4A^{iii}	102.5 (2)
F2—S1---F5	176.53 (10)	F4B—S1B---F4A^{iii}	79.92 (14)
F3—S1---F5	89.36 (9)	F9---S1B---F4A^{iii}	107.83 (7)
F4—S1---F5	94.69 (9)	F2C—S1C—F1C	100.49 (18)
F1—S1---F7^{i}	171.55 (9)	F2C—S1C—F3C	87.1 (2)
F2—S1---F7^{i}	81.81 (10)	F1C—S1C—F3C	90.0 (2)
F3—S1---F7^{i}	101.29 (10)	F2C—S1C—F4C	88.2 (2)
F4—S1---F7^{i}	85.50 (9)	F1C—S1C—F4C	87.69 (19)
F5---S1---F7^{i}	101.15 (8)	F3C—S1C—F4C	174.3 (3)
F1A—S1A—F2A	99.76 (15)	F2C—S1C---F4^{iv}	79.99 (13)
F1A—S1A—F3A	87.10 (15)	F1C—S1C---F4^{iv}	179.35 (14)
F2A—S1A—F3A	87.53 (13)	F3C—S1C---F4^{iv}	90.48 (14)
F1A—S1A—F4A	87.31 (15)	F4C—S1C---F4^{iv}	91.89 (14)
F2A—S1A—F4A	87.99 (13)	F2C—S1C---F4C^{v}	171.49 (17)
F3A—S1A—F4A	172.15 (14)	F1C—S1C---F4C^{v}	84.89 (15)
F1A—S1A---F8	76.09 (11)	F3C—S1C---F4C^{v}	86.32 (19)
F2A—S1A---F8	172.92 (11)	F4C—S1C---F4C^{v}	98.66 (11)
F3A—S1A---F8	97.89 (10)	F4^{iv}---S1C---F4C^{v}	94.68 (8)
F4A—S1A---F8	86.10 (10)	F6—S2—F10	86.74 (13)
F1A—S1A---F3A^{ii}	168.85 (12)	F6—S2—F9	85.13 (13)
F2A—S1A---F3A^{ii}	78.66 (11)	F10—S2—F9	89.98 (13)
F3A—S1A---F3A^{ii}	103.79 (8)	F6—S2—F7	85.99 (15)

F4A—S1A---F3A^{ii}	81.62 (11)	F10—S2—F7	90.35 (13)
F8---S1A---F3A^{ii}	104.29 (7)	F9—S2—F7	171.08 (13)
F2B—S1B—F1B	101.8 (2)	F6—S2—F8	83.96 (12)
F2B—S1B—F3B	88.5 (3)	F10—S2—F8	170.70 (13)
F1B—S1B—F3B	87.41 (18)	F9—S2—F8	88.89 (10)
F2B—S1B—F4B	88.8 (2)	F7—S2—F8	89.35 (11)
F1B—S1B—F4B	86.03 (18)	S2—F8---S1A	125.71 (10)
F3B—S1B—F4B	172.2 (2)	S2—F9---S1B	134.86 (12)

Symmetry codes: (i) x−1, y, z; (ii) x−1/2, −y+1/2, −z+1; (iii) x+1/2, −y+1/2, −z+1; (iv) x+1, y, z; (v) x+1/2, −y+1/2, −z.